MONKEYPOX

Multiple lineages of monkeypox virus detected in the United States, 2021–2022

Crystal M. Gigante[1], Bette Korber[2], Matthew H. Seabolt[1,3], Kimberly Wilkins[1], Whitni Davidson[1], Agam K. Rao[1], Hui Zhao[1], Todd G. Smith[1], Christine M. Hughes[1], Faisal Minhaj[1], Michelle A. Waltenburg[1], James Theiler[4], Sandra Smole[5], Glen R. Gallagher[5], David Blythe[6], Robert Myers[6], Joann Schulte[7], Joey Stringer[7], Philip Lee[8], Rafael M. Mendoza[9], LaToya A. Griffin-Thomas[10], Jenny Crain[11], Jade Murray[12], Annette Atkinson[12], Anthony H. Gonzalez[13], June Nash[13], Dhwani Batra[1], Inger Damon[1], Jennifer McQuiston[1], Christina L. Hutson[1], Andrea M. McCollum[1], Yu Li[1]*

Monkeypox is a viral zoonotic disease endemic in Central and West Africa. In May 2022, dozens of non-endemic countries reported hundreds of monkeypox cases, most with no epidemiological link to Africa. We identified two lineages of monkeypox virus (MPXV) among two 2021 and seven 2022 US monkeypox cases: the major 2022 outbreak variant called B.1 and a minor contemporaneously sampled variant called A.2. Analyses of mutations among these two variants revealed an extreme preference for GA-to-AA mutations indicative of human APOBEC3 cytosine deaminase activity among Clade IIb MPXV (previously West African, Nigeria) sampled since 2017. Such mutations were not enriched within other MPXV clades. These findings suggest that APOBEC3 editing may be a recurrent and a dominant driver of MPXV evolution within the current outbreak.

Monkeypox is a viral zoonotic disease caused by monkeypox virus (MPXV) that is endemic in West and Central Africa. There have been several reported cases of travel-associated monkeypox in non-African countries in recent years. In 2003, an outbreak of monkeypox in the United States was linked to imported African small mammals (*1*). In 2017, the largest monkeypox outbreak in western Africa occurred in Nigeria after decades of no identified cases (*2*), and during 2018 to 2021, eight cases were exported from Nigeria to non-endemic countries (*2*–*5*). In 2021, there were two US monkeypox cases in travelers from Nigeria, one in Maryland and one in Texas (*4*, *5*). In May of 2022, this pattern of monkeypox cases in travelers from Nigeria shifted. As of 28 September 2022, 67,602 cases of monkeypox were reported in 99 non-endemic countries, most with no epidemiological link to Africa (*6*), and 25,509 cases have been confirmed in the United States (*7*).

Comparison of MPXV sequences from nine US monkeypox cases from 2021 and 2022 (ON563414.3, ON674051, ON675438, ON676703, ON676704, ON676705, ON676706, ON676707, and ON676708) revealed two distinct lineages (Fig. 1) within MPXV Clade IIb (formerly named West African MPXV found east of the Dahomey Gap). Neutral nomenclature was chosen to reduce the stigmatization that can be associated with naming that is based on locations (*8*). We maintain the designation of two clades of MPXV, Clade I: formerly Congo Basin/Central African and Clade II: formerly West African, which are based on genetic distance and evidence-based clinical differences (*9*–*12*). Five of the seven May 2022 US sequences formed a monophyletic clade with 2022 MPXV sequences from Europe (Fig. 1), with most genomes within this clade containing zero to two nucleotide changes in nonrepeat regions (fig. S1 and table S1). This clade will be referred to as the current predominant 2022 MPXV outbreak variant, B.1 [which is based on proposed MPXV naming from Nextstrain (*13*)]. MPXV from a 2021 travel-associated case from Nigeria to Maryland (USA_2021_MD) displayed high similarity to variant B.1 sequences, with ~13 nucleotide differences (Fig. 1, fig. S1, and Table 1). The USA_2021_MD and 2022 outbreak sequences shared many mutations that separated them from MPXV sequences from Nigeria and travel-associated cases from 2017–2019 (table S2).

Two 2022 US MPXV sequences, USA_2022_FL001 and USA_2022_VA001, and one 2021 US sequence, USA_2021_TX, formed a monophyletic clade (variant A.2) that was polyphyletic to other 2022 MPXV sequences from the United States and Europe (Fig. 1). Each genome contained ~80 nucleotide changes relative to the variant B.1 MPXV sequences (fig. S1). The three variant A.2 genomes displayed ~30 unique nucleotide differences from each other (fig. S1 and table S3). Each case also reported travel to different countries in the Middle East and West Africa (table S4). This suggests that although the three MPXVs share a common ancestor, they likely represent separate introductions to the United States.

Real-time polymerase chain reaction (PCR) testing of USA_2021_MD and the five 2022 MPXV variant B.1 samples revealed a lower sensitivity (average Ct delay of 6.88, ranging from 5.3 to 8.3) in the *Orthopoxvirus* generic OPX3 real-time PCR assay (*14*) compared with the Monkeypox Clade II–specific real-time PCR assay (*15*) (table S5, when performed as described in Methods). By contrast, similar Ct values were observed for USA_2022_FL001, USA_2022_VA001, or USA_2021_TX samples (average difference of −0.78 Ct, ranging from −1.4 to 0.5). Careful comparison of Ct values between the two assays can, in theory, differentiate between cases belonging to variant B.1 and cases from other Clade IIb MPXV without sequencing. Sequence examination revealed a single nucleotide polymorphism (SNP) in the reverse primer-binding site for the OPX3 real-time PCR assay (DNA polymerase gene VACV-Cop E9L, C322T) in USA_2021_MD and variant B.1 sequences that was absent from other Clade IIb MPXV sequences. The decreased sensitivity in the OPX3 assay is unrelated to the US Food and Drug Administration–cleared VAC1 assay (*16*) used for MPXV screening. Use of different commercial reagents, run parameters, or PCR platforms may result in different results.

When we compared the 2022 outbreak MPXV sequences in Fig. 1 with other MPVX sequences in Lineage A, we noticed a marked preponderance of G-to-A mutations, specifically 5′ GA-to-AA or 5′ GG-to-AG, indicative of host Apolipoprotein B mRNA Editing Catalytic Polypeptide-like3 (APOBEC3) activity (*17*, *18*) (Fig. 2 and Table 2). Looking at this systematically, we found that a significant enrichment of APOBEC3 context G-to-A mutations was evident throughout Lineage A, among Clade IIb MPXV sequences sampled from 2017 to 2022 (Fig. 2 and Table 2). Overall, among unique mutations within Lineage A, 167 G-to-A mutations were in an APOBEC3 context, whereas nine G-to-A mutations were not in an APOBEC3 motif, and only 14 mutations were not G-to-A (Fig. 2 and Table 2). The vast majority of the APOBEC3 context G-to-A mutations were specifically GA-to-AA (156 of 167, or 95%; Fig. 2), indicating that if these mutations were generated by APOBEC3 editing, then APOBEC3G was not the major form because it produces GG-to-AG changes (*19*, *20*).

[1]National Center for Emerging and Zoonotic Infectious Diseases, Centers for Disease Control and Prevention, Atlanta, GA, USA. [2]T-6: Theoretical Biology and Biophysics, Los Alamos National Laboratory, Los Alamos, New Mexico, USA; New Mexico Consortium, Los Alamos, NM, USA. [3]Leidos Inc., Reston, VA 20190, USA. [4]ISR-3: Space Data Science and Systems, Los Alamos National Laboratory, Los Alamos, NM, USA. [5]Massachusetts Department of Public Health, Jamaica Plain, MA, USA. [6]Infectious Disease Epidemiology and Outbreak Response Bureau, Maryland Department of Health, Baltimore, MD, USA. [7]Dallas County Health and Human Services Public Health Laboratory, Dallas, Texas, USA. [8]Florida Department of Health Bureau of Public Health Laboratories-Jacksonville, Jacksonville, FL, USA. [9]Florida Department of Health in Broward County, Hollywood, FL, USA. [10]Virginia Department of General Services, Division of Consolidated Laboratory Services, Richmond, VA, USA. [11]Virginia Department of Health, Richmond, VA, USA. [12]Utah Department of Health and Human Services, Salt Lake City, UT, USA. [13]Sacramento County Public Health, Sacramento, CA, USA.
*Corresponding author. Email: yuli@cdc.gov

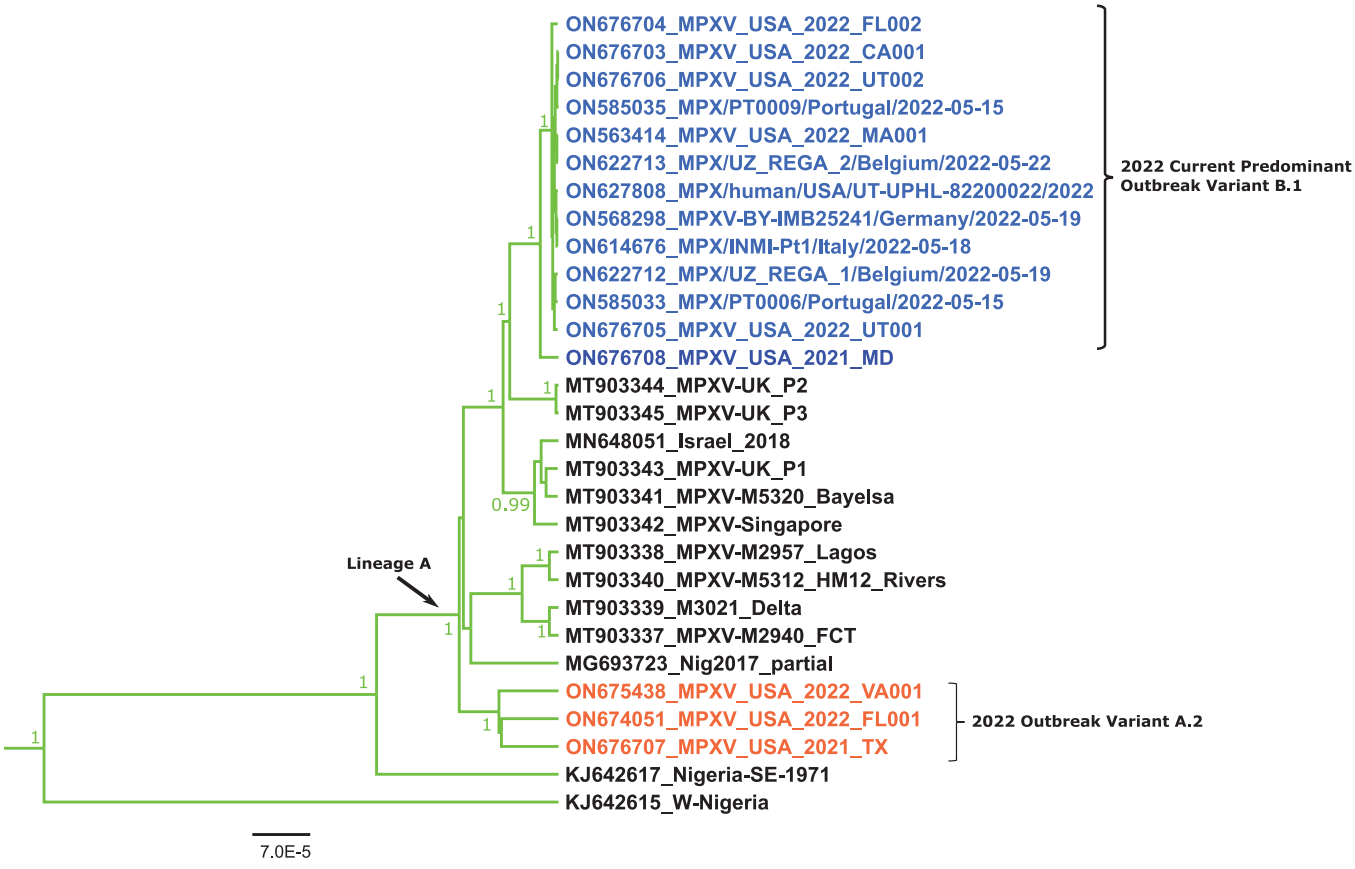

Fig. 1. Phylogenetic analysis of Clade IIb MPXV genome sequences. Variant B.1 sequences are shown in blue text, variant A.2 sequences in orange text, and green branches indicate Clade IIb. Phylogenetic analysis was performed in BEAST v1.8.3 using the HKY+G model and constant coalescent prior on complete genome alignments after removing all sites containing gaps. Scale bar is in substitutions per site; posterior support values are shown at branch points.

We explored the abundance of APOBEC3 motif G-to-A mutations along the evolutionary trajectory from the common ancestor of Lineage A to the variants A.2 and B.1 (Fig. 2 and fig. S2). The path from the estimated ancestor of Lineage A to the estimated ancestors of both variant B.1 and variant A.2, including each internal branch, revealed significantly increased APOBEC3 motif G-to-A changes, indicating that sequential acquisition of mutations in distinct individuals sampled historically since 2017 have contributed to the high proportions of GA-to-AA APOBEC3 (fig. S2 and table S6). Given the limited variation found in 2022 outbreak sequences in variant B.1, there were only a small number of SNPs relative to the ancestor for any one sequence. When considered together, however, all eight SNPs observed among the 12 variant B.1 genomes available in early May 2022 were GA-to-AA APOBEC3 context mutations (Fig. 2, fig. S2, and table S6). Outbreak-related sequence data have increased very rapidly, enabling the analysis of 397 outbreak genomes sampled between 1 May and 15 July 2022, available through the GISAID data sharing initiative (*21*). This greatly expanded dataset confirmed the pattern observed among

Table 1. Unique coding nucleotide changes in 2022 predominant MPXV outbreak variant B.1. Mutations listed (all SNPs) were shared among all MPXV Clade IIb variant B.1 sequences examined in Fig. 1 and were not present in USA_2021_MD or UK-P2 (MT903344.1). Gene homologs in vaccinia virus Copenhagen (VACV-Cop) are given for each gene. Additional information can be found in table S2.

Position*	MD 2021	2022 Outbreak	Effect	Amino acid change	Note
3120, 194114	G	A	Synonymous		VACV-Cop C19L ankyrin-like
39148	C	T	Missense	Glu353Lys	VACV-Cop F13L major envelope antigen of EEV
73248	G	A	Missense	Asp88Asn	VACV-Cop G8R VLTF-1 (late transcription factor 1)
74214	G	A	Missense	Met142Ile	VACV-Cop G9R entry/fusion complex component
77392	G	A	Missense	Glu162Lys	VACV-Cop L4R ss/dsDNA binding protein
84596	C	T	Synonymous		VACV-Cop J6R RNA polymerase subunit (RPO147)
150480	C	T	Missense	His221Tyr	VACV-Cop A46R IL-1/TLR signaling inhibitor
170273	G	A	Synonymous		VACV-Cop B12R Ser/Thr kinase
183534	C	T	Missense	Pro722Ser	VACV-Cop B21R membrane-associated glycoprotein

*Position in MT903344.1.

the first 12 sequences: 275/308 (89%) of observed unique G-to-A mutations occurred in an APOBEC3 context, and 261/275 (95%) of these were specifically 5′ GA-to-AA (Fig. 2, fig. S3, and table S7). Beyond variant B.1, by partitioning Lineage A into sublineages (A.2, Nigeria 2017, and Nigeria 2017–2019; Fig. 2) we found that G-to-A mutations in variant A.2 were in an APOBEC3 context and were enriched throughout Lineage A (Fig. 2, fig. S2, and table S6). Four additional MPXV sequences belonging to variant A.2 have now been detected in India and Thailand (*22*); 45/47 (96%) G-to-A mutations were in an APOBEC3 context, and all 45 of these were specifically 5′ GA-to-AA (table S7).

By contrast, APOBEC3 context G-to-A changes were lower than would be expected by chance relative to other G-to-A changes across Clade I and Clade IIa MPXV (Fig. 2, fig. S2, and table S8). To better resolve where within the phylogeny the switch in mutational patterns arose, we evaluated the mutational frequencies along the internal branches in Clade IIb leading into Lineage A (Fig. 2, fig. S2, and table S8), and these were not found to be statistically enriched for APOBEC3 context G-to-A changes.

In the 15 July 2022 GISAID sample, there were three highly related sequences, one each from Italy, Spain, and France. These were chimeric in that most of the genome was typical of variant B.1, but each inverted terminal repeat region carried five consecutive bases that were typically found among other Lineage A and Clade IIb MPXV, but not among B.1 sequences. A detailed analysis of these sequences is provided in fig. S4, and they were excluded from the analysis shown in fig. S3. This pattern is potentially indicative of recombination, an important aspect of poxvirus evolution (*23*); however, assembly errors caused by reference calling in low coverage regions could not be ruled out as a possible explanation.

Given the clear transition in the mutational pattern in Lineage A relative to Clades I and IIa (Fig. 2), we explored the hypothesis that there was a concomitant change in the evolutionary rate in Lineage A. First, we used the fixed local clock model as implemented in BEAST to compare the estimated mean evolutionary rate of Lineage A ($7.2 \times 10^{-6} \pm 8.9 \times 10^{-7}$ SD) with those of Clade I ($1.9 \times 10^{-6} \pm 3.1 \times 10^{-7}$ SD) and Clade IIa ($3.9 \times 10^{-6} \pm 8.9 \times 10^{-7}$ SD) (table S9). We also separated Lineage A, retaining Nigerian-SE-1971 as an outgroup, from Clade I and IIa and repeated the analysis using two trees. We felt this to be the more appropriate alternative given the transition in the underlying evolutionary model. In this analysis, we found that Lineage A had an even higher evolutionary rate estimate of $2.8 \times 10^{-5} \pm 8.8 \times 10^{-6}$ SD, whereas estimates for Clades I and IIa were essentially unchanged (table S9). Thus, using either approach, we observed higher evolutionary rates within Lineage A, consistent with mutations being driven by host editing mediated through APOBEC3 over what is expected by errors in the viral polymerase. An enriched evolutionary rate for Clade B.1 outbreak viruses has been similarly reported by others (*18*, *22*). A cautionary note regarding the robustness of estimates of rates of evolutionary change is that molecular clock assumptions may be violated in a scenario where

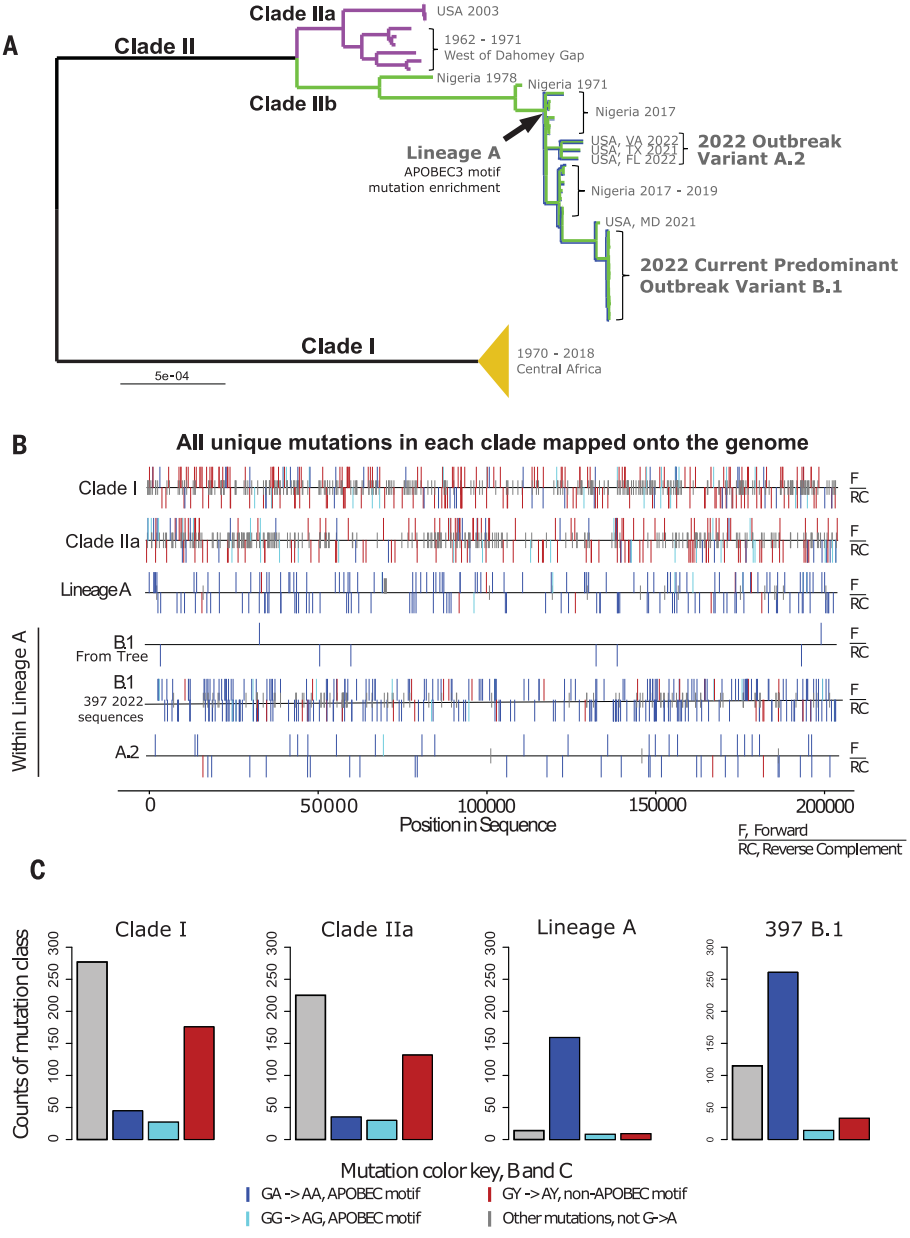

Fig. 2. Analysis of APOBEC3 motif mutations in MPXV. (**A**) Maximum likelihood phylogenetic tree using IQ-TREE. Enrichment for G-to-A APOBEC context mutations (blue line) was found in Lineage A, within Clade IIb (green branches). A detailed version of this tree with taxa names is included in fig. S2. The scale bar indicates the number of substitutions per sequence site. (**B**) Mutational patterns found among Clade I, Clade IIa, and Lineage A in the phylogeny above. All unique mutations in a clade relative to the most recent common ancestor of that clade are shown in a single panel, and the class of each mutation is shown on either the forward or reverse complement strand. The increased number of APOBEC3 context mutations, indicated by blue ticks, in Lineage A, versus red and gray captures the dominance of GA-to-AA APOBEC3 context mutations in this lineage and contrasts with Clades I and IIa. The exact numbers and statistics are provided in Table 2. The A.2 and B.1 variants within Lineage A in the tree and an updated analysis of 397 variant B.1 sequences from GISAID demonstrate the continuing dominance of GA-to-AA APOBEC3 context mutations among currently sampled outbreak sequences. (**C**) Bar charts showing the total number of each class of unique mutations within each clade shown in (B) for Clade I, Clade IIa, and lineage A, as well as for 397 sequences from lineage B.1 from fig. S3A.

Table 2. Summary of the counts of different classes of all unique mutations observed in the different clades shown in Fig. 2. C-to-T mutations in the forward strand are included as G-to-A in the reverse complement as a simplified way of tallying all mutations that occurred in the context of an APOBEC3 motif in the viral genome relative to those that did not. *P* values are derived from a Fisher's exact test of a contingency table based on columns 4 to 7. First, we identified all G's either in an APOBEC context (GA or GG) or not in an APOBEC context (GC or GT), and then we determined the number that had undergone G-to-A substitutions and the number where the G was unchanged within each of the two contexts. An ABOBEC motif odds ratio >1 indicates APOBEC context enrichment. The final column shows the number of GA-to-AA and GG-to-AG mutations that constitute the total G-to-A APOBEC context mutations in column 4.

	Clade	All other mutations	G-to-A APOBEC context	G in APOBEC context, no change	G-to-A non APOBEC context	G not in APOBEC context, no change	*P* value (two-sided)	*q* value	Odds ratio	GA-to-AA + GG-to-AG
Non-APOBEC context	I	277	72	36552	176	30580	<0.000001	0.000006	0.3423	45 + 27
	IIa	225	65	36548	132	30578	<0.000001	0.000006	0.412	35 + 30
APOBEC context enriched	Lineage A	14	167	36415	9	30669	<0.000001	0.000006	15.63	159 + 8
	B.1 (*n* = 12)	0	8	36517	0	30675	0.0095	0.022	Infinity	8 + 0
	B.1 (*n* = 397)	115	275	35064	33	29705	<0.000001	0.000006	7.06	261 + 14

mutations are dominated by host-mediated APOBEC3 deaminase activity, as different people may have different levels of APOBEC3 activity, and this may vary during the course of an infection. For example, transient increases in G-to-A ABOBEC3 motif–enriched mutations in HIV genomes in single infected hosts have been observed both in HIV-1 infection in humans and simian-HIV (SHIV) infections in monkeys (*24*, *25*)

All publicly available MPXV genomes from the 2022 monkeypox outbreak to date belong to Clade II, which may cause less severe disease and have a lower case fatality rate than Clade I MPXV (*10*–*13*). Genomes published during the 2022 outbreak share a common ancestor with MPXV sequences from Nigeria (Clade IIb); however, sequences from surrounding countries are limited, and most of our understanding of these relationships comes from viruses linked to or identified in Nigeria. The high similarity among the current predominant 2022 MPXV outbreak variant B.1 sequences analyzed here is similar to the 0.4 to 1.5 SNPs reported between genomes from epidemiologically linked samples from the same transmission chain (*3*). Among Clade IIb sequences, many unique mutations were shared between USA_2021_MD and variant B.1 genomes, further indicating that any evolutionary force leading to these changes most likely preceded the 2022 outbreak and were found in a common ancestor shared between the variant B.1 and USA_2021_MD. By contrast, there were sufficient differences (>30 SNPs) among the three variant A.2 sequences to suggest that they likely represent separate introductions into the United States.

After the reemergence of MPXV in Nigeria in 2017 and before 2022, there had only been two reported events of person-to-person transmission of MPXV outside of Africa (*3*, *26*). Several factors may be contributing to this recent increased spread between humans, including behaviors involving close contact and failure to recognize or diagnose monkeypox to prevent spread. It is currently unclear whether the APOBEC3 motif or other mutations observed in the 2022 outbreak MPXV variants have affected or will affect viral transmissibility or pathogenicity. An E353K mutation in F13L (which codes for the target of tecovirimat, an antiviral agent indicated for the treatment of smallpox) was shared by all sequences in the predominant 2022 outbreak cluster; functional studies revealed no effect on the efficacy of tecovirimat (the median effective concentration was 0.007731 ± 0.002 μM for 353E and 0.002860 ± 0.001 μM for 353K) (fig. S5).

APOBEC3 proteins are an important component of the vertebrate innate immune system and restrict the replication of exogenous viruses through cytosine-to-uracil deaminase activity (*19*, *27*). APOBEC3 proteins act mainly on single-stranded DNA and have been extensively studied in RNA viruses, including HIV (*20*), but can also act on DNA viruses (*28*, *29*). It is unlikely that the GA-to-AA substitutions we report here were caused by sequencing error because the sequences used in the analyses were produced across many different laboratories using multiple methods, including both short- and long-read approaches and with and without PCR. The presence of mutations consistent with APOBEC3 editing in several branches of the Clade IIb MPXV will cause discordance in estimates of evolutionary rate and divergence time using many standard methods.

Specific enrichment of the APOBEC3 motif mutations in Clade IIb MPXV since 2017 may suggest something different in virus-host interactions, facilitating this mutational pattern. Such a pattern might be caused by sustained transmission in a new host or a new route of infection. The APOBEC3 (A-to-G) locus carries seven genes or pseudogenes and is a primate-specific expansion of the APOBEC family of genes; APOBEC3 is not found in rodents (*30*), which are thought to be the primary reservoir of monkeypox virus in Africa. Additionally, APOBEC3 has been found at higher levels in mucosal tissues than in skin in humans (*31*), so permucosal transmission may provide increased opportunity for APOBEC3 editing of MPXV. Before this outbreak, APOBEC3 editing was not recognized or appreciated as a mechanism of poxvirus mutation. Two studies in vaccinia virus found that the overexpression of APOBEC3 had no effect on viral replication and that endogenous or overexpressed APOBEC3 was not degraded by vaccinia virus, as it is by other viruses (*32*, *33*). However, neither of these studies performed sequencing. The fact that the enrichment can be observed at essentially all levels within Clade IIb MPXV since 2017 suggests that it is a recurrent and dominant mutational effect in recent MPXV evolution. Furthermore, the majority of the mutations detected among expanding outbreak samples were 5′ GA-to-AA (Fig. 2 and table S7), indicating that this mutational bias is continuing.

REFERENCES AND NOTES

1. Centers for Disease Control and Prevention (CDC), *MMWR Morb. Mortal. Wkly. Rep.* **52**, 561–564 (2003).
2. A. Yinka-Ogunleye *et al.*, *Lancet Infect. Dis.* **19**, 872–879 (2019).
3. M. R. Mauldin *et al.*, *J. Infect. Dis.* **225**, 1367–1376 (2022).
4. V. Costello *et al.*, *Emerg. Infect. Dis.* **28**, 1002–1005 (2022).
5. A. K. Rao *et al.*, *MMWR Morb. Mortal. Wkly. Rep.* **71**, 509–516 (2022).
6. Centers for Disease Control and Prevention, "2022 global map & case count" (CDC, 2022); https://www.cdc.gov/poxvirus/monkeypox/response/2022/world-map.html.
7. Centers for Disease Control and Prevention, "2022 U.S. map & case count" (CDC, 2022); https://www.cdc.gov/poxvirus/monkeypox/response/2022/us-map.html.
8. C. Happi *et al.*, *PLOS Biol.* **20**, e3001769 (2022).
9. A. M. Likos *et al.*, *J. Gen. Virol.* **86**, 2661–2672 (2005).
10. K. Brown, P. A. Leggat, *Trop. Med. Infect. Dis.* **1**, 8 (2016).
11. M. G. Reynolds *et al.*, *Emerg. Infect. Dis.* **13**, 1332–1339 (2007).
12. C. L. Hutson *et al.*, *BioMed Res. Int.* **2015**, 965710 (2015).
13. J. Hadfield *et al.*, *Bioinformatics* **34**, 4121–4123 (2018).
14. M. G. Reynolds *et al.*, *Am. J. Trop. Med. Hyg.* **82**, 746–754 (2010).

15. Y. Li, H. Zhao, K. Wilkins, C. Hughes, I. K. Damon, *J. Virol. Methods* **169**, 223–227 (2010).
16. Y. Li, V. A. Olson, T. Laue, M. T. Laker, I. K. Damon, *J. Clin. Virol.* **36**, 194–203 (2006).
17. A. R. O'Toole, A. Rambaut, "Initial observations about putative APOBEC3 deaminase editing driving short-term evolution of MPXV since 2017" (Virological.org, 2022); https://virological.org/t/initial-observations-about-putative-apobec3-deaminase-editing-driving-short-term-evolution-of-mpxv-since-2017/830.
18. J. Isidro *et al*., *Nat. Med.* **28**, 1569–1572 (2022).
19. R. S. Harris, J. P. Dudley, *Virology* **479-480**, 131–145 (2015).
20. M. T. Liddament, W. L. Brown, A. J. Schumacher, R. S. Harris, *Curr. Biol.* **14**, 1385–1391 (2004).
21. GISAID, www.gisaid.org
22. B. Jolly, V. Scaria, *J. Infect.* **22**, 0.1016/j.jinf.2022.08.013 (2022).
23. J. J. Esposito *et al*., *Science* **313**, 807–812 (2006).
24. E. E. Giorgi, H. Li, T. Bhattacharya, G. M. Shaw, B. Korber, *mBio* **11**, e00324-e20 (2020).
25. B. F. Keele *et al*., *Proc. Natl. Acad. Sci. U.S.A.* **105**, 7552–7557 (2008).
26. G. Hobson *et al*., *Euro Surveill.* **26**, 2100745 (2021).
27. J. D. Salter, R. P. Bennett, H. C. Smith, *Trends Biochem. Sci.* **41**, 578–594 (2016).
28. J. P. Vartanian, D. Guétard, M. Henry, S. Wain-Hobson, *Science* **320**, 230–233 (2008).
29. J. P. Vartanian *et al*., *PLOS Pathog.* **6**, e1000928 (2010).
30. A. Jarmuz *et al*., *Genomics* **79**, 285–296 (2002).
31. C. J. Warren, K. Van Doorslaer, A. Pandey, J. M. Espinosa, D. Pyeon, *Virus Evol.* **1**, vev015 (2015).
32. M. Kremer *et al*., *Virol. J.* **3**, 86 (2006).
33. L. Soday *et al*., *Cell Rep.* **27**, 1920–1933.e7 (2019).
34. Sequence alignments for: C. M. Gigante, B. Korber, M. H. Seabolt, K. Wilkins, W. Davidson, A. K. Rao, H. Zhao, T. G. Smith, C. M. Hughes, F. Minhaj, M. A. Waltenburg, J. Theiler, S. Smole, G. R. Gallagher, D. Blythe, R. Myers, J. Schulte, J. Stringer, P. Lee, R. M. Mendoza, L. A. Griffin-Thomas, J. Crain, J. Murray, A. Atkinson, A. H. Gonzalez, J. Nash, D. Batra, I. Damon, J. McQuiston, C. L. Hutson, A. M. McCollum, Y. Li, Multiple lineages of monkeypox virus detected in the United States, 2021- 2022, Dryad (2022); https://doi.org/10.5061/dryad.jq2bvq8cd.
35. GISAID sequence alignment for: C. M. Gigante, B. Korber, M. H. Seabolt, K. Wilkins, W. Davidson, A. K. Rao, H. Zhao, T. G. Smith, C. M. Hughes, F. Minhaj, M. A. Waltenburg, J. Theiler, S. Smole, G. R. Gallagher, D. Blythe, R. Myers, J. Schulte, J. Stringer, P. Lee, R. M. Mendoza, L. A. Griffin-Thomas, J. Crain, J. Murray, A. Atkinson, A. H. Gonzalez, J. Nash, D. Batra, I. Damon, J. McQuiston, C. L. Hutson, A. M. McCollum, Y. Li, Multiple lineages of monkeypox virus detected in the United States, 2021- 2022, GISAID EpiPox Downloads (2022); https://doi.org/10.55876/gis8.220715bk.
36. Code used for APOBEC3 analysis for: C. M. Gigante, B. Korber, M. H. Seabolt, K. Wilkins, W. Davidson, A. K. Rao, H. Zhao, T. G. Smith, C. M. Hughes, F. Minhaj, M. A. Waltenburg, J. Theiler, S. Smole, G. R. Gallagher, D. Blythe, R. Myers, J. Schulte, J. Stringer, P. Lee, R. M. Mendoza, L. A. Griffin-Thomas, J. Crain, J. Murray, A. Atkinson, A. H. Gonzalez, J. Nash, D. Batra, I. Damon, J. McQuiston, C. L. Hutson, A. M. McCollum, Y. Li, Multiple lineages of monkeypox virus detected in the United States, 2021- 2022, Zenodo (2022); https://doi.org/10.5281/zenodo.6970457.

ACKNOWLEDGMENTS

We thank B. Foley for providing a draft alignment of MPXV; D. MacCannell, K. Patel, Y. Tao, S. Tong, B. Cherney, and J. Barnes from the US Centers for Disease Control and Prevention; A. Kim and S. Lukula from the Maryland Department of Health Laboratory; B. Downes from Fairfax County, Virginia Department of Health; C. Brown, L. Madoff, M. DeMartino, E. Buzby, S. Ash, and J. Hall from the Massachusetts Department of Health; J. Jaramillo from Dallas County LRN; D. Hairfield and K. Stratton from the Virginia Department of General Services, Division of Consolidated Laboratory Services; and the authors from the originating laboratories and the submitting laboratories who generated and shared the GISAID genetic sequence data on which this research is based (GISAID acknowledgments tables S10 and S11 are provided in the supplementary materials). **Funding:** No external funding was used for the Centers for Disease Control and Prevention (CDC) effort in this investigation. B.K. was supported by the Laboratory Directed Research and Development program of Los Alamos National Laboratory under project number 20220660ER. **Author contributions:** Conceptualization: Y.L., C.M.G., B.K., J.M., I.D.; Funding acquisition: Y.L., C.M.G., B.K.; Investigation: M.H.S., K.W., W.D., A.K.R., H.Z., C.M.H., F.M., M.A.W., J.T., S.S., G.R.G., D.B., R.M., J.S., P.L., R.M.M., L.A.G., J.C., J.M., A.A., A.H.G., J.N., D.B., A.M.M., T.G.S.; Methodology: Y.L., B.K., J.T., C.M.G., M.H.S.; Visualization: C.M.G., B.K., J.T., Y.L.; Writing – original draft: C.M.G., B.K.; Writing – review and editing: C.M.G., B.K., Y.L., I.D., A.M.M., C.L.H., J.M. **Competing interests:** The authors declare no competing interests. **Data and materials availability:** All data are available in the main text or public databases and GISAID. MPXV genomes were deposited to GenBank under accession numbers ON563414.3, ON674051, ON675438, ON676703, ON676704, ON676705, ON676706, ON676707, and ON676708. Alignments and code have been made available online (*34–36*).

SUPPLEMENTARY MATERIALS

science.org/doi/10.1126/science.add4153
Materials and Methods
Figs. S1 to S5
Tables S1 to S9
References (*37–43*)
MDAR Reproducibility Checklist
GISAID Acknowledgment Tables S10 and S11

View/request a protocol for this paper from *Bio-protocol*.

Submitted 12 June 2022; accepted 10 October 2022
Published online 20 October 2022
10.1126/science.add4153